Green Chemistry

Accepted Manuscript

ROYAL SOCIETY OF CHEMISTRY

www.rsc.org/greenchem

Green Chemistry

PERSPECTIVE

Towards sustainable fuels and chemicals through the electrochemical reduction of CO_2: lessons from water electrolysis

Received 00th January 20xx,
Accepted 00th January 20xx

DOI: 10.1039/x0xx00000x

www.rsc.org/

Antonio J. Martín, Gastón O. Larrazábal and Javier Pérez-Ramírez*

The storage of renewable energy through the electrochemical reduction of CO_2 (eCO_2RR) is an attractive strategy to transform the current linear utilisation of carbon fuels (extraction–combustion–CO_2 release) into an increasingly cyclic one. An electrochemical alternative for energy storage is the production of H_2 from water splitting, studied for decades and commercially available up to the megawatt range. By comparing the technological similarities between these two processes, it is possible to extract both a global perspective and research directions for the eCO_2RR. Herein, the main limiting phenomena affecting CO_2 electrolysers and their causes are outlined first. This is followed by the derivation, for several eCO_2RR products, of targets in terms of durability, current efficiency, energy efficiency, faradaic efficiency, and overvoltage, which must be achieved for the eCO_2RR to reach a similar energy storage capability as the electrochemical production of H_2. By comparing these figures of merit with the eCO_2RR literature, we conclude that the conversion of carbon dioxide to carbon monoxide and formic acid lead the race towards practical use, although both still exhibit major performance gaps. Present energy efficiencies are low, mainly due to high overvoltages, and durability is not yet a developed research area. Besides the development of more efficient electrocatalysts, research advances on the fronts of electrode and electrolyser design, coupled with the optimisation of methods for the preparation of electrodes, are expected to push forward the electrochemical reduction of CO_2 on its way to viability.

Introduction

The utilisation of CO_2 can be separated into two large categories: technological and enhanced biological utilisations.[1] Technological utilisation requiring the transformation of CO_2 can be in turn divided into two groups:[2] those in which carbon keeps its +4 oxidation state and those in which is reduced to +2 or lower (**Fig. 1**). The first group, aimed at the production of urea, polymeric materials, and inorganic carbonates, for example, includes reactions with low energy exchanges usually provided by reagents such as OH^-, amines, olefins, alkynes, and dienes. A catalyst is not always necessary, as in the cases of production of urea or salicylic acid. Typical products in the second group are HCOOH, CO, H_2CO, CH_3OH, or hydrocarbons. These reactions require higher energy exchanges provided by strong reducing reagents (H_2, metals) and/or electricity, heat, or radiation. Within this group, the presence of a catalyst is mandatory in the vast majority of cases. As a first approach, we may consider the products from the first group as chemicals and the products from the second group as fuels.[2] However, this is not a sharp division, since some reduced compounds such as CO, HCOOH, and H_2CO find use either as chemicals or as reactants for fuels production. The production of fuels from CO_2 is particularly attractive from economic and environmental standpoints, since the global market for fuels is 12-14 times larger than the market for chemicals.[1] On the other hand, the economic appeal of chemicals is based on smaller production volumes with high added value.

Efforts on the efficient reduction of CO_2 can be tracked down to the 19th century for formic acid production,[3] but only a reduced number of thermally-driven processes have become industrially viable; namely, the synthesis of methanol and the Sabatier reaction.[1] This raises the question of whether efficient reduction routes at low-temperature, powered by radiant or electrical energies, can be designed. Nature contains some positive examples: even though most plants transform only 1-2 % of the received solar radiation into chemical energy,[4] the theoretical maximum efficiency of photosynthesis is around 70 %. Although the evolutionary reasons for this are a matter of intense study, it is known that RuBisCO, the enzyme responsible in most plants for the carbon fixation step, is an inefficient catalyst.[5] Nevertheless, the impact of a more active enzyme may be mitigated by the limited availability of CO_2: assuming $[CO_2]$ = 400 ppm in the air and dark conditions for $t \leq 0$ s, the total depletion of CO_2 ($[CO_2]$ = 0 ppm) in a sunny day (solar irradiation of 1 kW·m^{-2}) with no wind (0.16 cm^2·s^{-1} as the diffusion coefficient of CO_2 in air[6]) would happen at the surface of a leaf at $t \cong 2$ s, considering a steady global energy efficiency of 2 % for the photosynthetic reaction[4] $nCO_2 + nH_2O \rightarrow (CH_2O)_n + nO_2$. Another example of a CO_2-reducing system can be found in bacteria living in volcanic

Institute for Chemical and Bioengineering, Department of Chemistry and Applied Biosciences, ETH Zurich, Vladimir-Prelog-Weg 1, CH-8093 Zurich, Switzerland. E-mail: jpr@chem.ethz.ch

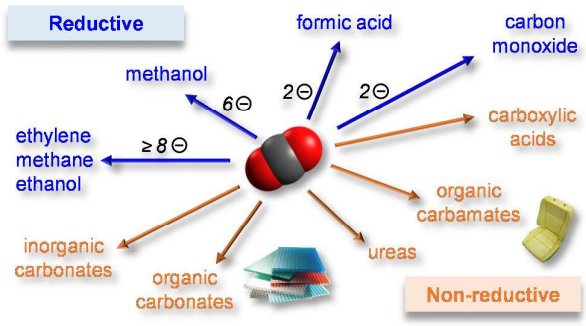

Fig. 1 The technological utilisation of CO_2 can be divided in those processes requiring low-energy exchanges, where carbon keeps its +4 oxidation state, and whose products are chemicals (Non-reductive),and those with high-energy exchanges, where carbon is reduced (electrons represented as minus signs in white circles) and whose products are fuels (reductive). Some compounds from the second group, such as CO, H_2CO, or HCOOH are widely used as chemicals but can be converted to fuels.

environments, which possess enzymes with very high activity for the CO_2/CO redox pair.[7–9] Practical catalytic processes for low-temperature CO_2 reduction are therefore a feasible objective.

Research on the electrochemical reduction of CO_2 powered by renewable electricity is justified by robust economic and environmental reasons. From a purely economic perspective, it shows potential for implementation at large scales,[10–12] with a predicted feasibility of the products decreasing according to the series $CO \approx HCOOH > CH_3OH >> C_2H_4 > CH_4$.[10] Agarwal *et al.*[11] conclude that, at the present stage of development, the operation of an electrochemical plant producing HCOOH at a cost around \$500 t^{-1} would require at least 25 years to reach profitability. It is interesting to note that, in this case, auxiliary processes such as CO_2 capture or distillation may be equally or more limiting than the energy consumption by electrolysers currently available.[11–15] Environmentally speaking, using emission-free energy sources is the only sensible approach to CO_2 recycling, apart from direct artificial photosynthesis, which is at an even earlier stage of development.[16]

Hydrogen production from water electrolysis and the electrochemical CO_2 reduction reaction (eCO_2RR) share several conceptual and technological features. The conceptual similarity comes from considering H_2 as a fuel in the context of the emerging *Hydrogen Economy*,[17] term coined in 1970.[18] They can therefore be seen as alternative technologies for storing electrical energy. Likewise, technological resemblances exist: both processes are cathodic in nature and the eCO_2RR is usually complemented by the oxygen evolution reaction (OER) in the anode. This leads to comparable designs for CO_2 and water electrolysers (or fuel cells), as reflected by the use of similar membranes, electrode types, bipolar plates, etc., as detailed later. From a more fundamental point of view, the similar standard reduction potential of the hydrogen evolution reaction (HER) and the eCO_2RR (**Table 1**), coupled to its much more simple and facile kinetics on a number of materials, make H_2 the most common undesirable product in CO_2-reducing experiments.[19] We can put forward that the knowledge attained on the electrokinetics of the HER may facilitate the development of efficient catalysts for the eCO_2RR capable of promoting required intermediate hydrogenation steps while hindering H_2 formation.

Currently, the stage of development of water splitting is more advanced,[20,21] as easily deduced by comparing the dozens of active projects up to the megawatt-scale based on the electrolysis of H_2O[22–26] with the few projects in the kilowatt-scale based on the reduction of CO_2.[10,15,27] Besides the inherent complexity of the eCO_2RR, a major reason for this is that the production of H_2 from renewable energies in alkaline or polymeric electrolyte membrane (PEM) electrolysers is a key component of a sustainable H_2-based framework. Its study has been boosted for decades by its incorporation into well-structured, multi-annual research programs in the U.S.,[28] Europe,[29] or Japan,[30] among other countries. Such programs analyse electrolysers, fuel cells, H_2 storage and transport technologies, and the required infrastructure to assess their short and long-term commercial feasibility. Among their outputs, a set of publicly available targets covering all key technological and economic parameters is of great importance as benchmarks for researchers and engineers. Two examples of such parameters are the cost of H_2, which targets \$2 kg^{-1} in 2020 from its current price of \$3.1 kg^{-1},[31] and the energy efficiency of electrolysers, to reach 78 % in 2020 from 76 % in 2015.[28] In the case of CO_2 conversion, no parallel framework based on a *CO_2 Economy* is in place, though the seminal and concrete idea of a *Methanol Economy* proposed by Olah exploits the same concepts.[32] Moreover, there is no clear set of target parameters in the literature for the eCO_2RR, which should be specific for each potential product due to their different nature and end uses.

In this work, we analyse the eCO_2RR from the perspective of a potential competing technology to water electrolysis based on their similarities. The identification and description of limiting phenomena for low-temperature CO_2 electrolysers is outlined first. This is followed by a set of proposed figures of merit for relevant products and how they compare with the current state of the art. Finally, some research directions for this process are proposed.

Table 1 Reduction potentials for electroreductions of CO_2 and hydrogen evolution reaction in alkaline aqueous solution versus the reversible hydrogen electrode. Potential for formate production is the only pH-dependent in the RHE scale (given at pH = 7). Other products such as n-propanol, acetaldehyde, acetate, and acetone have been detected to a much lesser extent.[51]

Cathodic half-reaction	E^0 *vs.* RHE (V)
$CO_2 + H_2O + 2e^- \rightarrow CO + 2OH^-$	-0.11
$CO_2 + H_2O + 2e^- \rightarrow HCOO^- + OH^-$	-0.03*
$CO_2 + 5H_2O + 6e^- \rightarrow CH_3OH + 6OH^-$	0.03
$CO_2 + 6H_2O + 8e^- \rightarrow CH_4 + 8OH^-$	0.17
$CO_2 + 8H_2O + 12e^- \rightarrow C_2H_4 + 12OH^-$	0.08
$2H_2O + 2e^- \rightarrow H_2 + 2OH^-$	0.00

*Under acidic conditions (pK_a = 3.77) the product would be HCOOH.

Limiting factors for the efficient electrochemical reduction of CO_2

The performance of an electrolyser is limited by factors of different nature.[33] Electrolyser design or thermodynamics impose inherent constraints, whereas other factors such as kinetics, power dissipation from the Joule effect, and mass transport limitations depend on the operating conditions and tend to increase the required cell voltage. The degradation of electrodes has a similar effect. The following paragraphs are devoted to the analysis of these factors and their related components for the case of the eCO_2RR.

Factors independent of the operating conditions

Thermodynamics

The Nernst cell voltage of a CO-producing electrolyser with OER as the anodic reaction ($E^0(H_2O/O_2)$ = 1.23 V *vs.* SHE) in standard conditions would be (−0.11) - 1.23 = -1.34 V (**Table 1**), corresponding to a ΔG = 257 kJ·mol^{-1} according to **equation (1)**,[34]

$$E^* = -\frac{\Delta G}{n\mathrm{F}} \quad (1)$$

where n is the number of electrons exchanged to form 1 mole of product, and F is the Faraday's constant. This value, however, is not necessarily the minimum theoretical cell voltage, because the enthalpy change between reactants and products is provided both by electricity and heat ($\Delta H = \Delta G + T\cdot\Delta S$). For endothermic reactions in electrolysers with no external heating system, the only available source of heat is the Joule effect. Thus, accounting for the entropic term requires the application of an additional overvoltage. Otherwise, the reaction would extract heat from the surroundings until the reaction stopped.

The thermoneutral voltage[35] E^n for endothermic systems is defined as the minimum voltage necessary to provide the required enthalpy change only through electrical energy, as shown in **equation (2)**.

$$E^n = -\frac{\Delta H}{n\mathrm{F}} \quad (2)$$

The calculation of overvoltages for CO_2 electrolysers must therefore be referred to the thermoneutral voltage when applicable. Any overvoltage over the thermodynamic minimum implies an excess power which is eventually dissipated as heat. Following the CO example, the global enthalpy change of the reaction $CO_2 \rightarrow CO + 0.5O_2$ is 283 kJ·mol^{-1}, consequently requiring an endothermic heat exchange of 26 kJ·mol^{-1}. Hence, the thermoneutral voltage is 1.47 V, which entails an overvoltage of 130 mV over the Nernst value regardless of kinetic considerations. **Table 2** reproduces these calculations for relevant CO_2 products, including the special case of syngas production (CO/H_2 = 1/1). Water splitting is also included for comparison. All global reactions in **Table 2** are endothermic, except for the case of formic acid, close to thermal neutrality. This is a special case, since its heat of dissociation should also be considered depending on the pH of the electrolyte. It must be noted that water splitting needs a considerably higher cell voltage than CO_2 reduction except for CO. From this, it follows that (i) at cell voltages $E^n(eCO_2RR) < E < E^n(HER)$, the HER rate would be severely limited and (ii) production of syngas in an eCO_2RR reactor is as efficient as separate productions of H_2 and CO from the thermodynamic point of view. From the kinetic point of view, however, producing hydrogen at the overpotentials typically needed for CO evolution would be energetically wasteful, since state-of-the-art catalysts are able to produce hydrogen at much lower overvoltages than CO. An interesting anodic reaction for fundamental studies on CO_2 electroreduction in electrolyzers may be the hydrogen oxidation reaction (HOR), due to its more facile kinetics than the OER. It allows to ascribe observed overpotentials almost entirely to the cathodic contribution, as it happens in PEMFCs. In that case, all reactions would be exothermic (global reactions are CO_2 hydrogenations), so the concept of thermoneutral voltage does not apply. Standard Nernst voltages would be those in **Table 1**.

Table 2 Standard Nernst (E^*) and thermoneutral (E^n) voltages for low-temperature electrolysers where the cathodic reaction is the reduction of CO_2 and the anodic one the oxygen evolution. Their difference is the overvoltage required to account for the entropic term of the global reaction

Products	Global reaction	E^* (V)	E^n (V)	$E^* - E^n$ (mV)
CO	$CO_2 \rightarrow CO + 0.5O_2$	1.33	1.47	134
HCOOH	$CO_2 + H_2O \rightarrow HCOOH + 0.5O_2$	1.34	1.34	0
CH_4	$CO_2 + 2H_2O \rightarrow CH_4 + 2O_2$	1.06	1.15	94
C_2H_4	$CO_2 + 2H_2O \rightarrow C_2H_4 + 3O_2$	1.15	1.22	69
CH_3OH	$CO_2 + 2H_2O \rightarrow CH_3OH + 2O_2$	1.21	1.25	41
C_2H_5OH	$2CO_2 + 3H_2O \rightarrow C_2H_5OH + 3O_2$	1.14	1.18	36
CO, H_2	$CO_2 + 2H_2O \rightarrow CO + H_2 + 0.5O_2$	1.28	1.47	193
H_2	$H_2O \rightarrow H_2 + 0.5O_2$	1.23	1.48	250

Electrolyser design

Even though relatively unimportant for laboratory-scale studies, the design of the electrolyser is crucial to the performance of any electrochemical process at a large scale. There is no standard, well-established configuration for CO_2 electrolysers. Several reactor concepts can be found in the literature, with most of them resembling the design of polymeric electrolyte membrane fuel cells (PEMFCs), in which the key element is a conducting membrane separating the cathodic from the anodic chambers.[36–39] **Fig. 2,** taken from Delacourt *et al.*,[39] contains the most frequently reported configurations. Other designs are less common, such as the microfluidic reactor used by the group of Kenis.[40,41] Designs including the transport of a species involved in the eCO_2RR are, in principle, the most efficient ones. The simplest alternative entails using a solid electrolyte for either H^+ or OH^- conduction (**Fig. 2a**). In this case, the sum of the anode and cathode reactions accounts for the global process. However, designs that include only solid electrolytes seem to present low

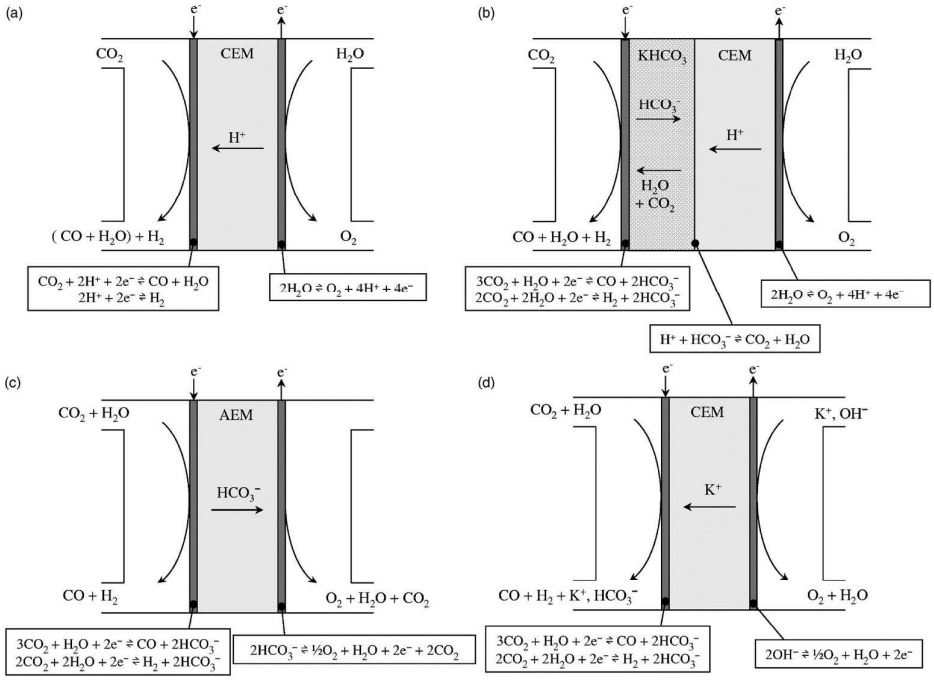

Fig. 2 Schematic representation of the most common membrane-containing configurations reported in the literature for the electrochemical reduction of CO_2, taken from Delacourt *et al.* (Ref 38). Copyright 2008. Reproduced with permission from The Electrochemical Society.

current efficiency for CO_2 reduction products.[39,42] This has been addressed by the addition of a liquid buffer layer, **Figure 2b**, which is equivalent in function to the solid electrolyte but unavoidably adds some ohmic resistance. On the other hand, designs including the transport of a species not directly involved in the eCO_2RR bring additional overvoltages regardless of the presence of a liquid buffer layer (**Figs. 2c** and **2d**). **Fig. 2c** shows how the transport of HCO_3^- through the membrane may be equivalent to a reduced solubility of CO_2 in the electrolyte, since only 1 out of 3 CO_2 molecules reaching the electrode react to form CO. The other two are transported to the anodic chamber to keep electroneutrality. This effect may explain apparent mass transport limitations observed by some authors.[38,43] If a cation-exchange membrane is used, **Fig. 2d**, the pH of the anodic chamber tends to decrease as the cathodic reaction progresses, steadily increasing both the pH difference between chambers and the required cell voltage when the cathodic and anodic electrolytes are not continuously replenished.[44]

Factors depending on the operating conditions

The anodic and cathodic contributions can be modelled as overvoltages to be added to the theoretical minimum cell voltage (either the thermoneutral or the Nernst one). This is shown in **equation (3)**,

$$E = E^n + \eta^{act} + \eta^{ohm} + \eta^{mt} \qquad (3)$$

where E stands for the cell voltage, η^{act} is the overvoltage due to anodic and cathodic kinetic activations, η^{mt} is the overvoltage due to limited mass transport in the anode and cathode, and η^{ohm} represents the overvoltage due to the presence of ohmic resistances. Different authors have modelled each term using diverse approaches.[19,45–47] Their relative influences vary at different operating conditions, as can be seen in a general current-voltage curve (**Fig. 3**). The performance is kinetically limited at low current densities and is usually well described by the Butler-Volmer or Tafel equations.[48] An almost linear response at higher currents is characteristic of predominant ohmic losses originated from the Joule effect, whereas mass transport limitation may arise at high current densities and is generally modelled by either the Fick's law or by the Pouseuille equation for multiphase flow in a specific pore network, when a more detailed description is needed.[49]

Kinetics

The main kinetic obstacles of the eCO_2RR are the large overpotentials and poor selectivity at industrially relevant current densities.[21] Since kinetics are largely determined by the electrocatalyst and the electrolyte, these two aspects will be discussed next.

Electrocatalyst: in spite of remarkable progress over the last decades towards practical systems, further research efforts are required. The incipient level of engineering is, at least in part, likely due to the current lack of industrially suitable catalysts. For instance, cathodic overpotentials are predominant in the eCO_2RR with the OER as the anodic reaction. The OER on iridium oxide catalysts can drive the cell

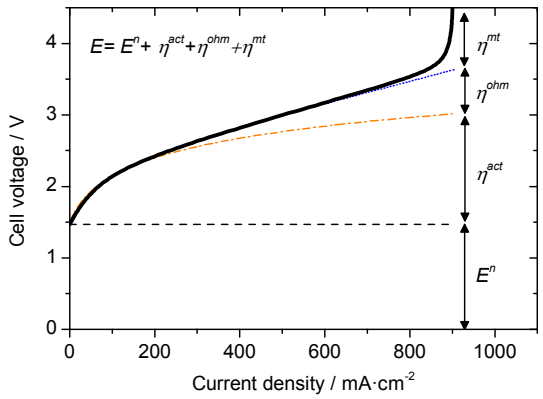

Fig. 3. An imaginary current-voltage curve for an electrolyser with CO production (cathode) and O_2 evolution (anode). As the current density increases the importance of the different limiting phenomena varies. For every point the total voltage is the sum of the thermoneutral voltage and the overvoltages. The orange dot-dashed and blue dotted lines correspond to the kinetic and to the ohmic contributions, respectively. The current becomes constant for pure mass transport limitations.

voltage of PEM water electrolysers to 1.6 V at 1000 mA·cm^{-2},[50] which is only 120 mV above the thermoneutral voltage of 1.48 V (**Table 2**). In regard to the eCO$_2$RR, transition and post-transition metals have been historically the most studied group of active materials.[51–53] However, they all show onset overvoltages on bulk surfaces larger than 300 mV. Some of them exhibit high selectivities for CO (Ag, Au) or HCOOH (Sn, Pb, In, Hg), whereas Cu has attracted the most interest due to its relatively high selectivity for hydrocarbons. Selectivities above 80 % in electrolyser tests have been obtained for CO and HCOOH using Ag and Sn catalysts, respectively, with H_2 as the main undesired product.[51]. The poor understanding of the nature of active sites and the insufficient knowledge on the reduction mechanism are major drawbacks for the design of new active and selective materials. CO_2 reduction comprises C-C and C-O bond breaking and formation steps,[54,55] mediated by multi- electron and proton transfers. In electrochemical environments, DFT studies on transition metals suggest the transfer of a ($H^+ + e^-$) pair at each elementary step.[9,54,56] Reaction pathways calculated this way match experimental data and predict limiting steps to become exergonic under lower overpotentials than under monoelectronic transfers (for the monoelectronic transfer, ($E^0(CO_2/CO_2^-)$ = -1.96 V *vs.* SHE,[57] whereas the concerted proton-electron transfer CO_2/COOH(ads) becomes exergonic at -0.41 V on copper[54]). Nonetheless, other materials such as oxides are known to be active through different mechanisms, such as the formation of CO_2^- [58] or a carbonate species,[59,60] for example. Open research lines such as the use of oxide-derived materials,[58,61–63] the role of metal-oxide interfaces,[64,65] the influence of ionic liquids and organic molecules as potential mediators and co-catalysts,[52,66–69] and the enhancement of the catalytic activity found in nanoparticulated materials due to size and composition effects.[70–73] are being developed in parallel with theoretical insights into the reaction mechanisms[9,54,55,74] (**Fig. 4**).

Electrolyte: to date, practical CO_2 electrolysis requires the use of a liquid electrolyte in the cathodic chamber, which, compared to PEM water electrolysers, implies an added complexity.[39,75] Mildly acidic or alkaline CO_2-saturated aqueous electrolytes containing inorganic salts with HCO_3^- or Cl^- as anions and alkali elements as cations (*e.g.* Na^+ or K^+) cover the vast majority of reported experiments. Nevertheless, the electrolyte is known to play a key role on the kinetics by altering the activity and selectivity: for instance, the choice of the cationic species alters the electric field into the double layer, altering the relative concentration of charged species close to the electrode.[76,77] Early works by Hori *et al.*[76] already showed how the cation choice between Li^+, Na^+, K^+, and Cs^+ profoundly impacts the selectivity on Cu electrodes, similarly to the case of Ag, where larger cations favour CO over H_2 production.[77] The choice of the anionic species, due to different buffer properties, influences the pH close to the electrode and therefore alters intermediate protonation reactions.[78] In this regard, a parallel work by Hori[79] with different anions (HCO_3^-, SO_4^{2-}, and Cl^-) also revealed different product distribution on Cu electrodes, confirmed by Wu *et al.*[80] for Sn.

Mass transport

This is a common limitation in electrochemical reactors operating at high current densities. CO_2 can reach the surface of the electrocatalyst either flowing through a porous medium or as a dissolved gas in a liquid electrolyte. A crucial limitation of the latter approach in aqueous solutions is that the content of free CO_2 is low, reaching about 30 mM in equilibrium with pure CO_2 at 1 bar and 25 °C. With such a low concentration, the limiting current density attainable is *ca.* i_L = 60 mA·cm^{-2} under vigorous stirring, according to the simple semi-infinite diffusion model[81] shown in **equation (4)**.

$$i_L = \frac{nFDC^*_{CO2}}{\delta} \qquad (4)$$

In this calculation, we considered a typical value for the diffusion coefficient[81] of $D = 1{\cdot}10^{-5}$ m^2·s^{-1}, a diffusion length of δ = 1 µm, and a bulk concentration of C^*_{CO2} = 30 mM for the case of CO production (n = 2). 60 mA·cm^{-2} is one order of magnitude below typical values found in industrial electrochemical reactors.[33,82] Taking this into account, it is clear that a simple design involving an aqueous electrolyte under ambient conditions would hardly result in a commercially viable reactor. Consequently, high pressures, stirring, and/or the use of different electrolytes, such as methanol, must be added to the picture in order to reduce mass transport overpotentials. Studies on the reduction of CO_2 at high pressures were mainly conducted in the 1990s by Sakata *et al.*,[83–85] and the use of non-aqueous media has been an active research topic for three decades.[86–89] The solubility of CO_2 in media such as methanol or ionic liquids is several orders of magnitude higher than in water, *e.g.* the equilibrium concentration of CO_2 in a methanol-CO_2 mixture at 40 bar is around 8 M at 25 °C,[90] equivalent to a limiting current density

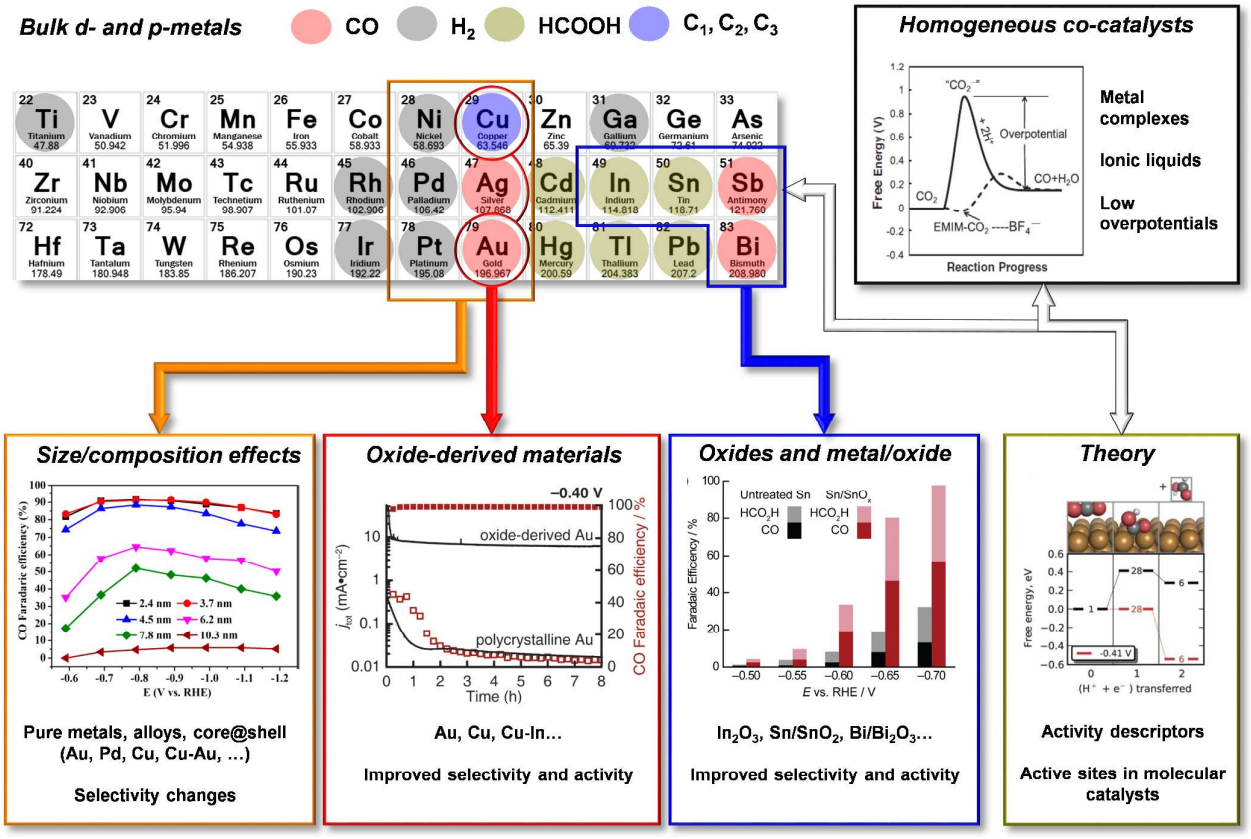

Fig. 4. Main research directions on new electroactive materials for the eCO_2RR. Most of them are based on the discovery of catalytic activity on bulk d-and p-metals in the 1980s. Nanoparticles and alloys can show very different catalytic properties compared to bulk metals (**size/composition effects**). Fig reproduce how selectivity to CO changes along with size of Pd nanoparticles. Some oxides as precursor materials result in highly active and selective catalysts (**oxide derived catalysts**). Fig. reproduces activity and faradaic efficiencies for oxide-derived gold compare with bulk. Some oxides and oxide/metal are highly selective catalysts (**oxides and metal/oxide**). Fig. shows improved selectivity to CO_2 reduction of Sn/SnO_2 *vs.* Sn. These figures are reprinted with permission from references 58, 64, and 71. Copyright 2015, 2012, 2012, respectively. American Chemical Society. Some metal complexes and ionic liquids play the role of potential mediators or co-catalysts, reducing CO_2 at low overpotentials (**homogeneous co-catalysts**). Fig. shows the effect of EMIM-BF_4 on the kinetic barrier of CO_2^- (from reference 66. Reprinted with permission from AAAS). DFT studies work in parallel with experimental findings to elucidate some reaction mechanisms and activity descriptors. (**Theory**). Fig. shows the proposed pathway for HCOOH formation on Cu, taken from reference 54.

of 16 000 mA·cm^{-2} (**equation (4)**). Interestingly, current densities up to 500 mA·cm^{-2} with moderate faradaic efficiencies (46 %) have been reported under these conditions.[91] However, the use of non-aqueous solvents carries its own set of cost and sustainability issues.[92]

The alternative, that is, the direct flow of gaseous CO_2 to the catalytic surface, is achieved by the use of a gas diffusion electrode (GDE) similar to those found in low-temperature fuel cells and water electrolysers. A GDE consists of stacked porous layers, namely, a commercial gas diffusion layer (a 100-400 μm thick carbonaceous paper or cloth with 65-80 % porosity), a microporous layer (10-40 μm, 30-50 % porosity), and a catalytic layer (> 10 μm). CO_2 is fed from the back of the electrode and reacts at sites where CO_2, electrons, and protons (or water) meet, which are known as the triple phase boundary[93,94] (**Fig. 5**). Therefore, GDEs must show high electronic conductivity, allow a high accessibility for reacting species, and favour the efficient removal of the formed products. In light of these considerations, the proper design of a GDE entails a complex optimisation problem with multiphase physics that has received constant attention over decades.[19,95,96] Currently, this approach renders negligible η^{mt} (**Fig. 3**) in H_2 devices at practical current densities. In particular, the design of an optimized GDE for the eCO_2RR should also include the gaseous or liquid nature of the target product and whether it is to be removed by backflow towards the back of the electrode or by "dumping" directly into the electrolyte. Electrolysers for eCO2RR using GDEs have reached remarkable current densities of around 200 mA·cm^{-2} even at room temperature and ambient pressure.[36,39,97]

Dissipation of heat from the Joule effect

Ohmic resistances from non-perfect electro- and ion-conductors cause the dissipation of electrical power in the form of heat due to the Joule effect. Current and overvoltage are linked by Ohm's law, described in one dimension by **equation (5)**.

$$i = -\sigma_t \frac{d\eta}{dx} \quad (5)$$

σ_t is the electronic or ionic conductivity and x the spatial coordinate. For a given conductivity, it predicts a linear variation of the overpotential at constant current. This regime describes with enough accuracy the membrane, electrolyte, and the gas diffusion and microporous layers, as well as the electron-conducting components. The total ohmic resistance of a cell is highly dependent on a number of factors, such as the assembling procedure, humidification degree of the membrane, or the operation temperature, but it is independent of the chemical reactions. It is routinely measured on-line as the value of the impedance with zero imaginary component at frequencies above 1 kHz, obtained by electrochemical impedance spectroscopy (EIS). Out of ionic and electronic contributions, the ionic resistance is the largest one. As an example, a Nafion® 112 membrane shows an optimum protonic conductivity[98] of 10 $S \cdot m^{-1}$ (comparable to a 10 % w/w $KHCO_3$ solution,[99] 7 $S \cdot m^{-1}$), whereas the electronic conductivity of stainless steel reaches 1.4×10^6 $S \cdot m^{-1}$. In PEMFCs and PEM electrolysers, most of the power dissipation occurs in the membrane: at 1000 $mA \cdot cm^{-2}$, Nafion® 112 (thickness of $5 \cdot 10^{-3}$ cm^{-2}) dissipates 51 $mW \cdot cm^{-2}$, which is equivalent to η^{ohm} = 51 mV. In a CO_2 electrolyser, the presence of a liquid electrolyte chamber is expected to provoke larger overvoltages. For instance, Kopljar *et al.*[100] operated their cell at 100 $mA \cdot cm^{-2}$ with $\eta^{ohm} \approx 950$ mV.

Equation (5) predicts a more complex picture in a porous catalytic layer (**Fig. 5**). Both the electronic current density and the conductivity vary locally. As a practical result, the ionic resistance of the catalyst layer becomes an important contribution to the total one.[19] This resistance is estimated from EIS by fitting experimental data to refined finite transmission line models (TLM).[101,102] In the case of PEMFCs and PEM electrolysers, the addition of 20-25 % of ionomer to the catalytic ink seems to reach an optimum compromise between the conduction of protons, the flow of other reactants, and the hydrophilic character of the resulting layer. Regarding the preparation method, deposition of catalyst inks on membranes, called the *decal* method, has proved to be valid for minimizing this resistance.[103,104] Typical ionic conductivities of catalyst layers are around 2 $S \cdot m^{-1}$ in Pt/C cathodes for PEMFCs.[102] In CO_2 electrolysers with electrolyte chamber, higher conductivities are expected. However, there are no reported values in the literature to our knowledge.

Degradation

Research on fuel cells and water electrolysers led to the identification of several degradation mechanisms, most of them directly applicable to CO_2 electrolysers.[105–107] The degradation of the membrane is one of the main reasons for shortened lifetimes. There are three identified degradation mechanisms for commonly used perfluorosulfonated acid membranes (PFSA): mechanical, thermal, and (electro)chemical degradation.[106] The first one is due to cracks,

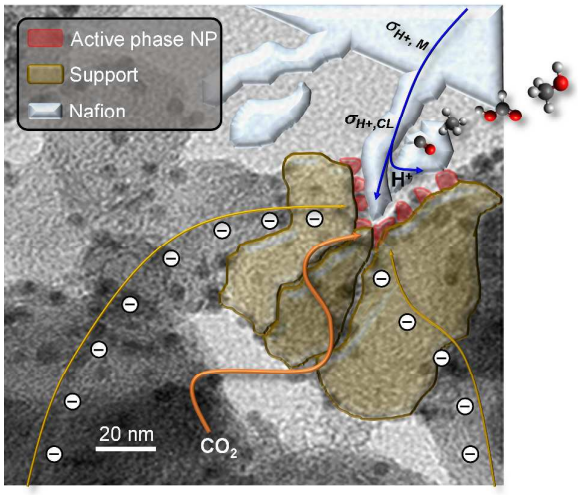

Fig. 5. Scheme based on a TEM image of a cathodic catalyst layer in a GDE for CO_2 reduction, formed by a supported nanoparticulated material with Nafion as the ion-conducting phase. Active particles (red) are only those at triple-phase boundaries, where protons, electrons, and CO_2 meet. The relatively low protonic conductivities of the membrane ($\sigma_{H+,M}$) and the catalytic layer ($\sigma_{H+,CL}$) typically account for the vast majority of the total ohmic resistance of the cell

tears, or pinholes as a consequence of hydration cycles, during which in-plane shrinkage (low humidification) and expansion (high humidification) occur. This results in the crossover of reactants between the anodic and the cathodic chambers, which is especially harmful if the oxidizing and the reducing agents can exothermically react as in PEMFCs. The thermal mechanism is associated to critical breakdown due to the glass transition of fully hydrated membranes at temperatures above 80 °C.[108] Its origin is normally a locally high current density, which creates a hot spot due to the Joule effect. Edge effects at corners or borders, or using a non-optimized catalytic deposition method are common causes.[106,109] The (electro)chemical degradation arises either from the presence of radicals (mainly HO• and HOO•), created by certain compounds such as hydrogen peroxide,[105–107] or by attack of foreign cations M^+, which cause M^+/H^+ exchange in the terminal group $R\text{-}SO_3^-H^+$ to yield $R\text{-}SO_3^-M^+$, with the consequence of a dramatic reduction in conductivity.[110] Among cations with affinity for sulfonic groups, Fe^{x+}, Ni^{x+}, and Cr^{x+} are present in stainless steels used for reactors and piping. In a CO_2 electrolyser, the membrane would be usually in contact with water, assuring a proper humidification, however, certain impurities arising mainly from "dirty" CO_2 sources (**Table 3**) are likely to be present, as described below.

The slow degradation of the gas diffusion and microporous layers of a GDE due to the decomposition of PTFE, at high temperatures and high oxygen concentrations, is manifested as an increase of the hydrophilicity, although this effect is not considered to be critical.[107,111,112] In contrast, the catalytic layer is much more sensitive to degradation. Supported nanoparticulated active materials suffer from particle coarsening, corrosion of the support, and poisoning: nanoparticles may dissolve in the ionomer phase and

Table 4 Main impurities in CO_2 streams from natural gas power plants and manufacturing of Portland cement after carbon capture units. Air components are supposed to be eliminated in the carbon capture units.

	Natural gas (ppm)	Portland cement (ppm)
CO	800	1600
N_2O	20	0
NO_X	2300	3300
HCl	0	65
SO_2	5	4400
TOC	90	80

redeposit on the surface of large particles (Ostwald ripening), or agglomerate due to their high surface energy. In PEMFCs, coarsening of particles takes place during the first hundreds hours of operation, causing a decrease of the electrochemically active area up to 50 % and the loss of most undercoordinated sites typically encountered in nanoparticles.[112–114] Another common phenomenon is the corrosion of the support,[105,106,115] favoured by high temperatures, high water content, low pH, high oxygen concentrations, and high voltages.[105,107] Out of these factors, only a high water content would be present in the cathodic environment of a CO_2 electrolyser, but the anodic OER takes place under very aggressive conditions due to the combination of oxygen, water, and high voltages. According to Roen *et al.,*[116] the oxidation rate of carbon supports according to the reaction $C + 2H_2O \rightarrow CO_2 + 4H^+ + 4e^-$ ($E^0 = 0.207$ V *vs* RHE) is negligible below 1.1 V due to slow kinetics. However, the presence of a catalyst such as Pt reduced the threshold to 0.55 V. When the support is corroded, not only its chemical properties and hydrophilicity change,[117] but a loss of electrocatalytic material occurs due to its detachment and dissolution into the electrolyte.[106] The third factor, poisoning, can be relevant even at trace levels of certain impurities, as low as 10 ppb of H_2S for Pt in the case of the HER, for example.[118] The presence of poisoning agents stems from corrosion of the metallic body of the reactor or piping, undesired (electro)chemical reactions, or the use of not pure reactants. Most metallic cations present in the cathodic electrolyte under eCO_2RR will undergo reduction on the surface of the catalyst and, since almost all reduced metals show activity towards CO_2 or H_2O reduction, such deposits will lead to activity and/or selectivity changes. A concentration as low as 50 nM (Fe^{2+}) has been claimed to be the reason for Cu deactivation after just 1 hour.[119] Besides, reaction products can remain strongly adsorbed on the surface of the catalyst and block active sites, as is the case of CO on Pt,[120] the proposed presence of CH_2O on Ag,[121] or graphite on Cu.[122] Interestingly, in the latter report, authors claim the presence of Cu_2O on the surface of Cu avoided the formation of graphite and allowed for continuous electrolysis. However, a clear source of impurities for the eCO2RR is the origin of the CO_2. Some processes provide extremely pure CO_2 such as fermentation, but those appropriate for large-scale CO_2 reduction, such as the flue gases from cement production or natural gas power plants, produce impurities above trace levels which are not trapped in carbon dioxide capture units (**Table 3**).[123] Except CO, all of them are potentially detrimental for the eCO2RR: nitrogen oxides may undergo preferential reduction to ammonia under typical cathodic voltages,[124] which is a well-known CO_2 capture agent. Special attention must be paid to the presence of sulphur due to its strong adsorption on numerous metals. So far, very limited reports on the influence of these contaminants on the eCO_2RR are available. For instances, exposure to Na_2S led to a decreased selectivity to CO on Ag[125] or to CH_4 on Cu[126] (from 36 % to 2 %), though CO selectivity increased on a Zn electrode (from 15 % to 44 %).[126] Consequently, understanding the impact of impurities and the quantification of allowed maximum levels in CO_2 streams remain as pending tasks.

Figures of merit

Qualitatively, an efficient eCO_2RR requires highly active, stable, and selective catalysts operating in electrolysers with both low ohmic resistance and high mass transport properties. The quantification of these features is much more difficult. Although there are several parameters to characterize the performance of an electrochemical system, its practical viability depends on a few key concepts, namely, the current density, the durability, and the energy efficiency.

Current density

It is defined as the current flowing divided by the geometrical area of the electrode. It is dependent, for a fixed potential, on the intrinsic activity, load, and utilisation of the catalyst, the transport rate of reactants, and the removal rate of products. Current densities for electrosynthesis reactors are usually above 1000 $mA \cdot cm^{-2}$ for selectivities close to 50 %,[33] and from 500 to 600 $mA \cdot cm^{-2}$ for highly selective electrolyses, such as the chlor-alkali process.[82] Electrochemical water splitting in PEM electrolysers is an outstanding case which typically shows both high selectivity and high current density: 1400 $mA \cdot cm^{-2}$ is achieved at moderate overvoltages with > 90 % selectivity.[19]

When H_2[127] and products from the eCO_2RR are considered as fuels —either directly or as reactants for subsequent

Table 3 Values of energy storage as chemical energy based on the LHV for various products of the eCO_2RR per coulomb transferred, $E_{C,i}$. CDH_2 refers to the required current density to obtain the same rate of energy storage compared to an electrode producing hydrogen at 1000 $mA \cdot cm^{-2}$.

Products	LHV ($kJ \cdot mol^{-1}$)	$E_{C,i}$ ($kJ \cdot C^{-1}$)	$E_{C,H2}/E_{C,i}$ (-)	CDH_2 ($mA \cdot cm^{-2}$)
CO	283.0	142	1.01	1010
HCOOH	254.6	127	1.12	1125
CH_4	890.3	111	1.28	1290
C_2H_4	1410.8	118	1.22	1220
CH_3OH	726.2	121	1.18	1180
C_2H_5OH	1367.3	114	1.26	1260
H_2	286.1	143	1.00	1000

synthesis processes like Fischer-Tropsch— the rate of energy storage becomes an important criterion for comparison. Considering a current density j for H_2 production, the equivalent current density for the eCO_2RR can be derived as follows: each produced mole of H_2 requires the transfer of 2 mol of electrons, and its lower heating value (LHV) is 286 kJ·mol^{-1}. Therefore, each coulomb stores $E_{C,H2}$ = 143 kJ of electrical energy as chemical energy. Similarly, for each produced mole of CH_4, 8 C are required and its LHV is 890 kJ·mol^{-1}, giving a value of $E_{C,CH4}$ = 111 kJ·C^{-1}. As a result, an electrode producing CH_4 should provide $E_{C,H2}/E_{C,CH4}$ = 1.28 times higher current density, or be *ca*. 30 % larger, than the one producing H_2 in order to have the same rate of electrical energy storage. From this perspective, j mA·cm^{-2} devoted to H_2 production are equivalent to 1.28·j mA·cm^{-2} for CH_4. **Table 4** contains $E_{C,i}$ for other relevant products and shows that all of them require higher current densities than H_2. $E_{C,H2}/E_{C,i}$ seems to rise with the number of electrons transferred (see **Table 1**), which suggests that first electronic transfers in the reduction process are more efficient in terms of energy storage. Considering 1000 mA·cm^{-2} as a representative value for PEM electrolysers, a similar eCO_2RR electrode would need to provide CDH_2 mA·cm^{-2} (= 1000·$E_{C,H2}/E_{C,i}$) (**Table 4**). The alternative of a larger electrode operated at a lower current density is not optimal from the point of view of the capital cost. Hence, we consider CDH_2 values as figures of merit for current density. Please note these are not total but partial reduction current densities.

Durability

This is probably the least studied aspect in the eCO_2RR literature. The gradual degradation of the electrode is accompanied by increasing overvoltages and eventual downtime once replacement becomes necessary. Despite the importance of this factor to the large-scale viability of the eCO_2RR, there are neither publications dealing with long-term stability tests (hundreds of hours) nor standardised stability test protocols. This fact points towards the existence of an almost unexplored field. It must be noted, however, that some efforts have been made to understand the mechanism behind the loss of activity of copper-based electrocatalysts during short tests.[119,128,129] Some studies highlight the importance of the operation mode, as revealed by the enhanced stability of the catalytic performance when a potential program including periodic anodic pulses in potentiostatic electrolyses was applied.[129,130]

Durability for electrosynthesis reactors is usually measured in years,[131] with examples such as the chlor-alkali process, where electrodes typically operate for 3 to 4 years before replacement.[82,107] Stability targets for electrodes with a steady decline of their performance are defined as the maximum rate at which the cell voltage is allowed to increase over time, as is the case for PEM electrolysers, whose typical degradation rates are below 15·mV·every 1000 h^{-1}.[132] The nature of the working load strongly influences durability: stationary fuel cells have proven lifetimes as high as 40 000 h, whereas an ambitious target for automotive fuel cells, whose load fluctuates to a large degree, is 5000 h.[28] Regarding water splitting electrolysers, advanced alkaline and PEM types show outstanding operation times beyond 20 000 h under mild conditions,[19,133,134] though they are reported to be very sensitive to factors such as the anodic catalyst load.[135] Following the parallelism with H_2 technologies, these figures suggest CO_2 electrolysers will probably need to reach lifetimes in the range of thousands of hours under typical cycling loads from renewable energy sources. We consider 5000 h as a first cornerstone for this figure of merit.

Energy efficiency

It is defined as the ratio between the energy stored in the desired products and the applied electrical energy. The definition of energy efficiency includes the concepts of overvoltage and faradaic efficiency. The overvoltage is the potential difference between the thermodynamically determined cell voltage and the observed experimentally, whereas the faradaic efficiency/current efficiency/selectivity for a given product i accounts for the fraction of the total charge used for its production, defined in **Equation (6**),

$$\varepsilon_{f,i} = \frac{n_i m_i \mathrm{F}}{Q} \quad (6)$$

where n_i is the number of electrons transferred per molecule of product i, m_i is the amount of mole formed, and Q the total charge passed in C. The energy efficiency is thus calculated with **equation (7)**,

$$\varepsilon_e = \sum_i \frac{E_i^n \varepsilon_{f,i}}{E_i^n + \eta_i} \quad (7)$$

Where E_i^n is the thermoneutral or Nernst cell voltage for the product i. It should be noted that $E_i^n + \eta_i$ equals the total cell voltage. Consequently, the reasons for low energy efficiencies are high overvoltages (energy wasted as dissipated heat) and/or low selectivity (energy wasted as undesired products). The energy efficiency of electrochemical water splitting technologies can routinely reach values over 70 %.[28,131,133] The global energy efficiency of methanol synthesis by catalytic hydrogenation of CO_2 with electrochemically produced H_2 (*i.e.* another green CO_2 conversion process) is around 50 %.[2] Its high catalytic efficiency suggests this value as a reliable reference for other CO_2 hydrogenations based on electrochemical hydrogen. Hence, a viable eCO_2RR must show an efficiency higher than 50 % to compete favourably. However, imposing a target of 70 %, similar to H_2 production, is demanding in terms of overpotentials for a process where very high selectivity is rarely obtained: for CH_4, **equation (6)** predicts a cell overvoltage of 164 mV at 80 % selectivity. A more realistic value of 400 mV would result in 59 % energy efficiency. We thereby consider 60 % for CO_2 reduction products as a figure of merit with more attainable overvoltage and selectivity requirements. We must note this figure might be finely tuned for each product according to its typical faradaic efficiency, but

here it is considered as the common reference for the sake of simplicity. **Fig. 6a** shows the maximum cell overvoltages allowed to reach 60 % energy efficiency under standard conditions for relevant eCO_2RR products. As an example, the maximum allowed cell overvoltage for CH_3OH at 90 % selectivity would be around 600 mV. High faradaic efficiencies tolerate relatively high overvoltages (*i.e.* over 600 mV), whereas a lower (though still high) value of 70 %, already imposes very restrictive conditions (*ca.* 200 mV). **Fig. 6b** separates the influences of the overvoltage and faradaic efficiency for the CO_2 reduction to CO. The energy efficiency for compounds with lower thermoneutral potentials, like CH_4, is more sensitive to variations in the cell overvoltage, as can be seen by comparing the dashed line (CH_4) with the solid one (CO) at the same selectivity of 80 %. From the point of view of the process, the faradaic efficiency not only influences the energy efficiency, but is also a critical parameter in determining the capital and operating costs. High values are desirable to reduce both the need of subsequent separation units and the energy requirements, but largely reduce the number of valid catalytic systems for this process. We propose 80 % as a figure of merit requiring reasonable overvoltages of around 400 mV, according to **Fig. 6a.**

The sum of cathodic and anodic half-cell overpotentials equals the cell overvoltage, but usually only cathodic half-cell overpotentials for eCO_2RR are available in the literature. Nevertheless, at low and moderate current densities they can be considered as cell overvoltages with acceptable accuracy, since the OER displays a low half-cell overpotential under these conditions. For example, cell voltages for electrochemical water splitting in the literature average 1.52 V[19,50,136] at 200 mA·cm^{-2}, which is only 40 mV over the thermoneutral potential (**Table 2**). Therefore, 40 mV is the maximum half-cell overpotential that can be assigned to the OER at 200 mA·cm^{-2} (equivalent to assigning perfect kinetics to the cathodic HER). Since the vast majority of reports on eCO_2RR show lower current densities, the corresponding OER half-cell overpotential would only account for a few millivolts.

As a summary, **Table 5** contains the set of values considered in this work as figures of merit for relevant CO_2 reduction products: current density (CD_{H2}), durability, energy efficiency, faradaic efficiencies, and maximum cell overvoltage ($\eta_{80\%}$). State-of-the-art parameters for H_2 production are added for comparison. We must highlight this analysis is focused on the production stage. For the subsequent transport fand storage phases, production of carbon compounds is more advantageous due to their higher volumetric densities (*e.g.* CH_4 9 GJ·m^{-3}, C_2H_5OH 17 GJ·m^{-3}) than hydrogen (0.1 GJ·m^{-3}) A global analysis might therefore provide less demanding requirements for CO_2 reduction. Once limiting factors are described and target parameters proposed, the next section compares the state of the art of the eCO_2RR with figures in **Table 5** and proposes research directions to shorten the way curve towards feasible systems.

Current status and potential improvements

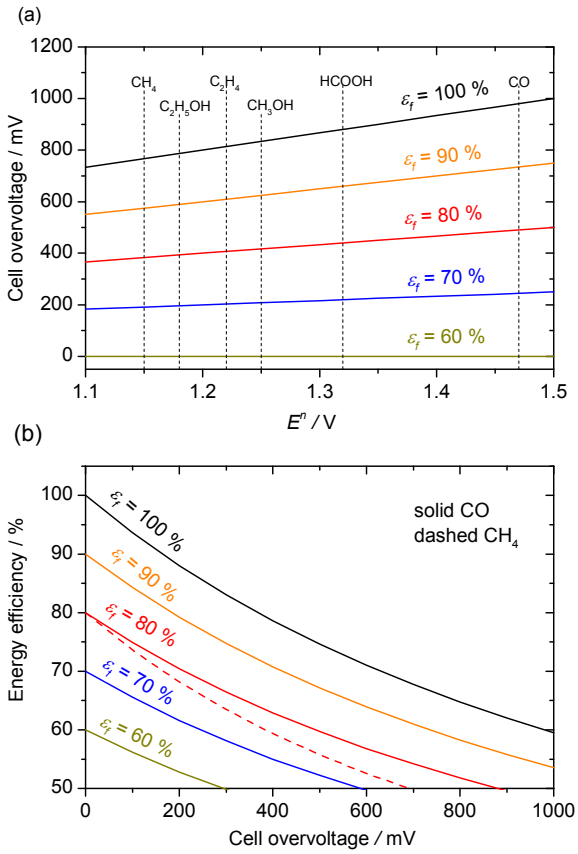

Fig. 6 (a) Maximum allowed cell overvoltages *vs.* standard thermoneutral potentials for different values of faradaic efficiencies at 60 % energy efficiency. (b) For the case of CO production, energy efficiency *vs.* cell overvoltage for different faradaic efficiencies. For comparison, the dashed line shows the case for 80 % faradaic efficiency for CH_4.

Current status

Fig. 7 aims to convey how targets in **Table 5** compare with the current status of the eCO_2RR. For each product, a representative report of the state of the art is plotted, with preference for those carried out in electrolysers at high current density and with good selectivity. Each axis of the pentagonal radar graphs ends at the corresponding value of **Table 5**. When a reported value from literature exceeds the upper limit of its axis, it is represented as equal to this limit, as an indication of a reached target (*e.g.* selectivities higher than 80 % are plotted as 80 %). For originally reported values see **Table 6**. An electrolyser reaching or surpassing all figures of merit would thus cover the entire pentagonal area.

Carbon monoxide

Kenis *et al.*[40] showed how joining benchmark catalysts for both the OER and the eCO_2RR in a microfluidic reactor, after carefully selecting the electrolyte and minimizing ohmic resistances, leads to an improved system for the electrochemical production of CO with high energy efficiencies and current densities over 100 mA·cm^{-2}. This system, whose performance is shown in **Fig. 7,** shows very high selectivity

Table 5 Considered minimum figures of merit for the eCO_2RR with OER as the anodic process to be competitive with water electrolysis. Energy efficiency (E.E.), current efficiency (C.E.), and cell overvoltage ($\eta_{80\%}$) are not independent, see text. $\eta_{100\%}$ represents the maximum cell overvoltage allowed at 100 % faradaic efficiency to comply with 60 % energy efficiency. Cell overvoltages are calculated with the standard thermoneutral potential. State of the art for H_2 electrochemical production from water splitting is added for comparison.

Products	CD_{H2} ($mA \cdot cm^{-2}$)	Durability (h)	E.E. (%)	C.E. (%)	$\eta_{80\%}$ (mV)	$\eta_{100\%}$ (mV)
CO	1010	5000	60	80	489	978
HCOOH	1125	5000	60	80	440	880
CH_4	1290	5000	60	80	384	769
C_2H_4	1220	5000	60	80	406	812
CH_3OH	1180	5000	60	80	418	836
C_2H_5OH	1260	5000	60	80	394	787
H_2	> 1600	20 000	70-75	> 90	120*	-

* Typical overpotential at 1000 $mA \cdot cm^{-2}$

(> 90 %) but large overvoltages. They also reported a remarkably low onset overvoltage of 20 mV for CO (operation point not plotted). Additionally, an example of a pressurised system reported by Hara and coworkers[137] with high selectivity and energy efficiency is plotted (blue patterned filling), in which the energy efficiency is increased due to a lower overvoltage. Other experiments at high pressure which are not plotted, such as the one reported by Dufek *et al.*,[97] reached higher current densities (225 $mA \cdot cm^{-2}$ at 80 % current efficiency) at 20 bar and 90°C, but with a lower energy efficiency of 50 %, similarly to Saeki *et al.*[91], who used CH_3OH as a solvent. We must highlight the outstanding CO partial current density of 3000 $mA \cdot cm^{-2}$ at 70 % current efficiency reported by Hara and coworkers[137] at 30 bar in aqueous solution. Unfortunately, the energy efficiency cannot be estimated as the cell voltage was not reported.

Formic acid

Sn catalysts have shown the best performance in electrolysers so far. Results from Oloman *et al.*[13] are plotted. A remarkable net current density of 225 $mA \cdot cm^{-2}$ was reported, but the energy efficiency was low due to high overvoltages. Recently, a report from Kopljar *et al.*[100] included very similar values in spite of high ohmic losses. Regarding pressurised systems, Todoroki and coworkers[84] successfully reached a notably high partial current density of 560 $mA \cdot cm^{-2}$ at 60 bar in aqueous solution with 90 % selectivity. Again, the lack of cell voltages in the report prevents any further analyses.

Hydrocarbons and alcohols

To the best of our knowledge, the production of methane, ethylene, methanol, and ethanol outside the laboratory scale has not been widely studied. Typically, current densities are low. For methane, a high current efficiency close to 80 % with an energy efficiency of around 40 % were recently reported by Manthiram *et al.*[138] A close case is ethylene, which has shown a high current efficiency (79 %) but low energy efficiency

Table 6 Representative reports of the state of the art for the electrochemical reduction of CO_2 depicted in Fig. 7.

Product	Stab. (h)	C.D. ($mA \cdot cm^{-2}$)	E.E. (%)	C. E. (%)	Overv. (mV)	Ref.
CO	5	135	50	80	980	[40]
	1	258	60	86	630	[137]*
HCOOH	4	195	20	65	2900	[13]
CH_4	1	8	39	77	1100	[138]
C_2H_4	5	36	29	79	2000	[139]
CH_3OH	1	0.2	87	98	150	[141]
C_2H_5OH	3	35	9.5	17	950	[142]

* 20 bar

(29 %) and current density (36 $mA \cdot cm^{-2}$).[139] In another report, Cook *et al.*[140] applied very high overvoltages (*ca.* 3000 mV) to achieve high partial current densities (280 $mA \cdot cm^{-2}$). As for liquid alcohols, excellent energy efficiency (87 %) and selectivity (98 %) for methanol were achieved by Arai *et al.*[141] at the expense of extremely low current densities, whereas only poor current and energy efficiencies have been reached for ethanol production.[142]

The analysis of **Fig. 7** clearly reveals that only the electrochemical reduction of CO_2 to CO and HCOOH currently exhibit current densities higher than 100 $mA \cdot cm^{-2}$, which is a promising value but still is far away from maturity. The beneficial effect of using pressurised systems is also noticeable. In general, operation times only account for a few hours, and energy efficiencies over 50 % and current densities higher than 100 $mA \cdot cm^{-2}$ are not simultaneously reached. Nevertheless, we must recall the optimisation of these systems is a multiparametric problem in a field which is still relatively young. Current catalysts operating under optimized conditions (in terms of pressure, temperature, electrolyte, etc.) in engineered electrolysers with low ohmic resistance and high mass transport properties would likely be much more efficient.

Potential improvements

We identify three main research areas in which remarkable developments in eCO_2RR electrolysers may be achieved. The analysis of auxiliary operation units and equipment needed to complete a full process for electrochemical CO_2 reduction are out of the scope of this contribution and are highly dependent on the product considered and the design of the electrolyser.

Catalysts

Maximum acceptable cell overvoltages at *ca.* 1000 $mA \cdot cm^{-2}$ for the eCO_2RR are around 400 mV (**Table 5**). To date, this is a very demanding condition even no overvoltage for the OER counterpart is assumed. Half-cell overvoltages below 300 mV induce no measurable activity on most known catalysts,[51] and measured current densities are far too low even in catalytic systems reported to be highly active at low overpotentials.[40,58,63,66] Taking this into account, it is clear that activity is a key pending challenge. Apart from Cu-based materials, selective catalysts for hydrocarbons and alcohols are

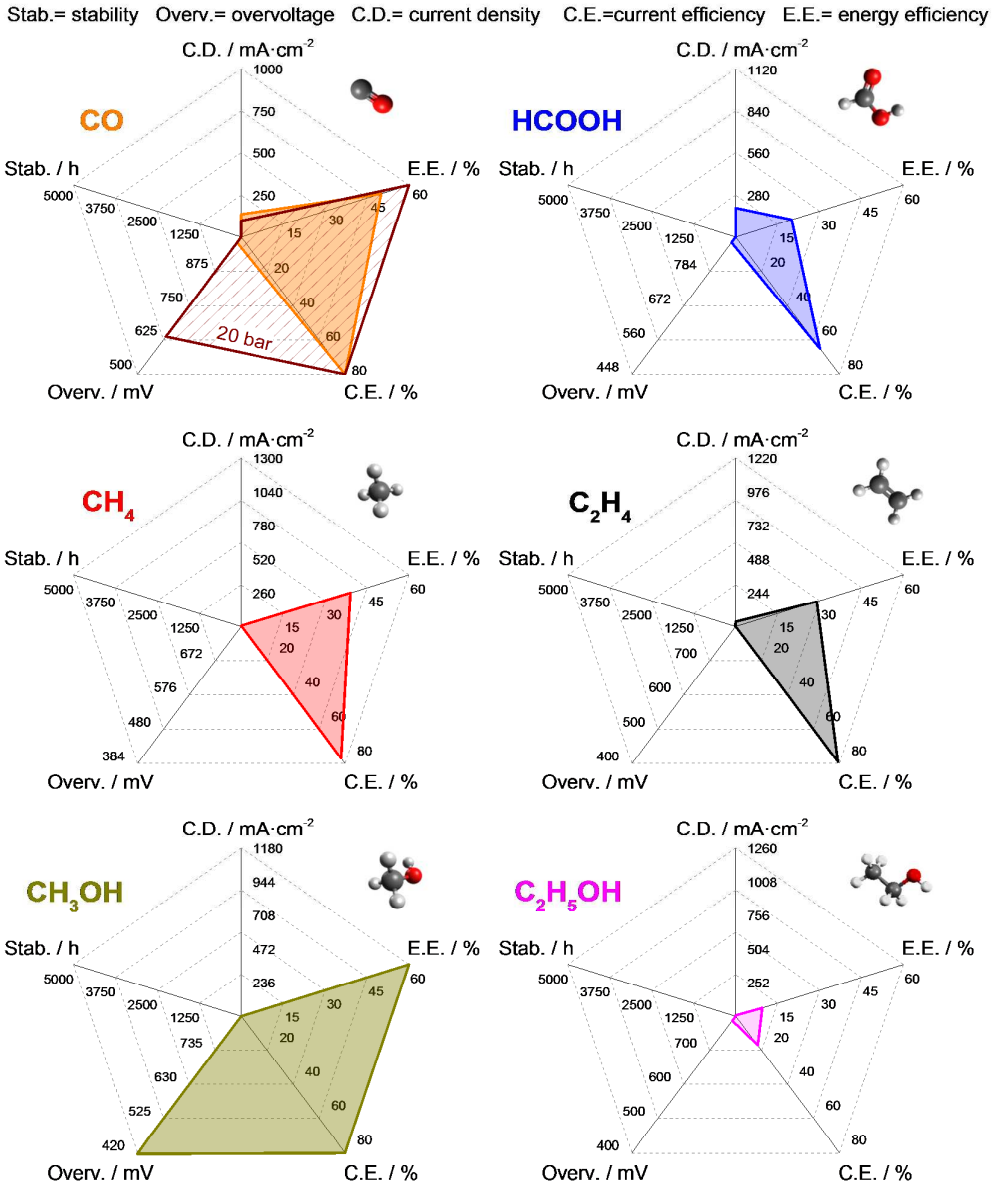

Fig. 7. Representative reports of the state of the art for relevant products from the eCO_2RR with respect to figures of merit in Table 5. Overvoltage values are given in standard conditions. Overvoltage axis start at the maximum overvoltage at 100 % selectivity ($\eta_{100\%}$), see Table 5. Among similar reports, those with higher current densities and faradaic efficiencies were selected. When only half-cell overpotentials are available, they have been taken as cell overvoltages (see text)

rare,[142–145] except for the case of CH_3OH, which is the main product on a few semiconductors[146,147] and oxides.[148] Durability tests longer than 10 hours are seldom found in literature,[11,149] as most known catalysts tend to quickly deactivate. Hence, we put forward that durability tests will gain notoriety as catalysts achieve better activities and selectivities. All in all, challenges in activity, selectivity, and durability are still present, as these parameters reflect plenty of room for improvement.

Electrodes

An evidence of the early stage of development of this technology is that research efforts on improving the performance of 'real-life' electrodes are still well behind those put on new active materials. This is in contrast to PEM fuel cells and electrolysers, in which a deeper understanding of structure-performance relationships from the micro to the nanoscale has increasingly attracted research efforts over the last decade.[150–153] At the microscale, the modelling of catalyst layers[154–157] predicts operation regimes which are far from straightforward, as they depend not only on the composition and structure of said layer but also markedly on operation conditions.[154,155] At low currents, the reaction rate and the

overvoltage are approximately constant across the catalyst layer (typically l_{cl} = 10-100 μm) and the polarization curve shows the expected Tafel slope. In contrast, at high currents and with η^{mt} as predominant, the regime changes: (i) the electrochemical conversion domain shrinks to a fraction of the catalyst layer, located close to the interface with the GDL, which is inversely proportional to the current density ($l^* \propto 1/i$, $l^* < l_{cl}$), and (ii) the polarization curve shows a double Tafel slope, therefore doubling the electrical power necessary to increase the current density one order of magnitude. An analogue situation arises when η^{ohm} is limiting but l^* is near the interface with the membrane, as depicted in **Fig. 8**. Besides, in this latter case, the overpotential is no longer constant within l_{cl}, a particularly important effect in the eCO_2RR in which selectivity and overvoltage are commonly strongly related. Typical l^* at relevant current densities are 10-15 μm for fuel cells. For PEMFCs, $l^* \leq l_{cl}$, but for direct methanol fuel cells (DMFC), $l^* << l_{cl}$.[154] At smaller scales, models on the influence of micro- and mesoporous structures on mass transport limitations revealed contributions from different transport phenomena, *e.g.* the significant contribution of around 40 % coming from Knudsen diffusion into catalytic aggregates larger than 100 nm,[156] which are typically found in Pt/C/ionomer layers. Down to the active site scale, experiments[158] and theory[159] describing the triple-phase boundary assign a surprising Pt effectiveness factor in PEMFCs below 5 %. In spite of the similarities, to the best of our knowledge there has been no attempt to apply these approaches to gain insight into electrodes for the eCO_2RR.

Even more abundant is the experimental work on the optimisation of catalytic layers for fuel cells based on variables such as the catalyst loading,[160] the cationic resistance,[161,162] and the optimum concentration of ionomers,[163] among others. In contrast, only a very limited amount of similar studies for the eCO_2RR are available.[36,164–166] An extensive set of reports is also available for the microporous layer in PEM electrolysers and fuel cells, aimed at the optimisation of key properties such as the pore size distribution and the composition, for example.[167,168] In this context, there is a great opportunity to further refine the structural understanding of practical electrodes at the meso- and macroscales by applying advanced visualisation techniques originally developed for technical heterogeneous catalysts.[36,169]

Preparation methods

The importance of the preparation method of membrane-electrode assemblies (MEA) in fuel cells and water electrolysers has been known for decades,[150,157,170] as the accessibility of reactants and stability of the catalyst markedly depend on it.[94] Several methods, such as brushing, electrospraying, catalyst-coated membranes (*decal*), electro-deposition, and electron-beam reduction, among others, are all well studied. Catalysts for the eCO_2RR are usually deposited on the surface of microporous layers, with little control of the final catalytic structure, either by impregnation of metallic salts followed by reduction or deposit of unsupported nanoparticles.[36,66] Deposition of supported catalysts

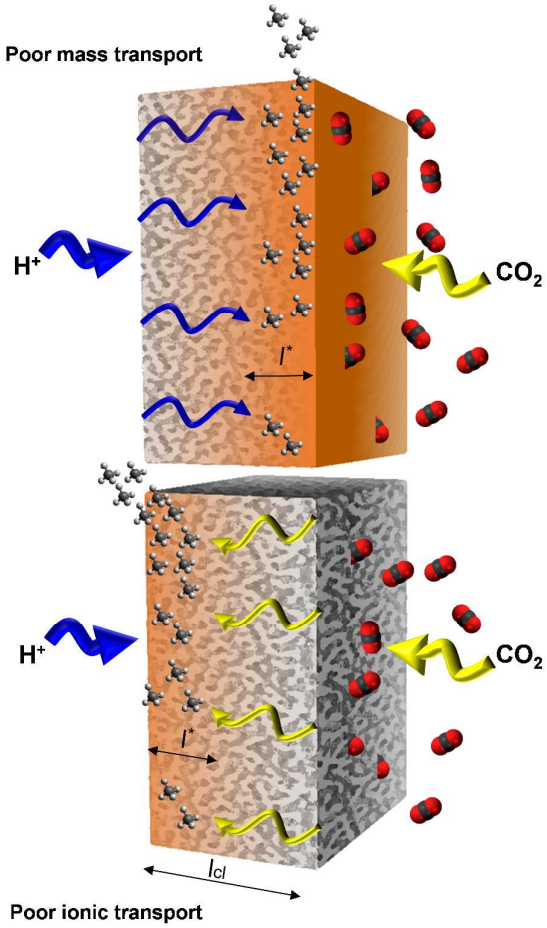

Fig. 8 Models for generic catalyst layers predict a non-homogeneous distribution of the reaction rate over the catalyst layer (l_{cl}) under certain conditions. If either the mass or ionic transport is poor, only a fraction of the catalyst layer (l^*) close to the microporous layer or membrane, respectively, is predicted to be active. Production of CH_4 is depicted as an example

suspended in catalytic inks, as is the standard procedure for H_2 devices, is a minority practice.[171] Only very recently, papers systematically exploring the influence of deposition methods for the eCO_2RR have started to appear.[36,100] For instance, Jhong *et al.*[36] found a dramatic enhancement on the current density for CO production when an automatised catalyst deposition method replaced the previous manual procedure, and claimed a higher performance sensitivity than similar electrodes for fuel cells. All in all, systematic studies of this kind in the context of the eCO_2RR are still lacking.

Conclusions and outlook

This work proposes a first set of figures of merit for different products from the electrochemical reduction of CO_2, aiming towards competitiveness with the electrolysis of water. Our analysis is based on their joint character as technologies capable of storing renewable energy and on the numerous technical similarities shared by both processes. The set of proposed parameters includes current density (around 1000 -

1300 mA·cm^{-2}), energy efficiency (60 %), current efficiency (80 %), overvoltage (400 – 500 mV), and durability (5000 h). By comparing these figures with representative reports in the literature we conclude that the production of CO and HCOOH are currently the only eCO_2RR processes with current densities close to industrial application, even though still far from required values. C_2H_4 and CH_4 show a similar degree of development, which is a step ahead of the production of CH_3OH or C_2H_5OH. In general, good current efficiencies have been reported, but energy efficiencies are still low due to high overvoltages. On the other hand, durability is not yet a developed research area. Besides the development of more efficient electrocatalysts, research advances on the fronts of electrode and electrolyser design and the optimisation of methods for the preparation of electrodes are expected to bring the electrochemical reduction of CO_2 a step forward on the road towards practical feasibility.

Acknowledgements

This work was financially supported by ETH Zurich (Research Grant ETH-01 14-1).

References

1 M. Aresta, A. Dibenedetto and A. Angelini, *Chem. Rev.*, 2014, **114**, 1709–1742.
2 M. Aresta, A. Dibenedetto and A. Angelini, *Phil. Trans. R. Soc. A*, 2013, **371**, 20120111–20120119.
3 M.E. Royer, *C. R. Hebd. Seances Acad. Sci.*, 1870, 731–732.
4 R. Govindjee, in *Energetics of Photosynthesis*, Academic Press, 1975, 1–50.
5 R. J. Spreitzer and M. E. Salvucci, *Annu. Rev. Plant Biol.*, 2002, **53**, 449–475.
6 T. R. Marrero and T. A. Mason, *J. Phys. Chem. Ref. Data*, 1972, **1**, 3–118.
7 J.-H. Jeoung and H. Dobbek, *Science*, 2007, **318**, 1461–1464.
8 Y. Kung and C. L. Drennan, *Curr. Opin. Chem. Biol.*, 2011, **15**, 276–283.
9 H. A. Hansen, J. B. Varley, A. A. Peterson and J. K. Nørskov, *J. Phys. Chem. Lett.*, 2013, **4**, 388–392.
10 N. Sridhar, A. Agarwal and E. Rode, *Electrochemical Production of Chemicals*, 2012.
11 A. S. Agarwal, Y. Zhai, D. Hill and N. Sridhar, *ChemSusChem*, 2011, **4**, 1301–1310.
12 A. Dominguez-Ramos, B. Singh, X. Zhang, E. G. Hertwich and A. Irabien, *J. Clean. Prod.*, 2013, **104**, 148–155.
13 C. Oloman and H. Li, *ChemSusChem*, 2008, **1**, 385–391.
14 H. Li and C. Oloman, *J. Appl. Electrochem.*, 2007, **37**, 1107–1117.
15 X. Lu, D. Y. C. Leung, H. Wang, M. K. H. Leung and J. Xuan, *ChemElectroChem*, 2014, **1**, 836–849.
16 E. V. Kondratenko, G. Mul, J. Baltrusaitis, G. O. Larrazábal and J. Pérez-Ramírez, *Energy Environ. Sci.*, 2013, **6**, 3112–3135.
17 J. M. Bockris and A. J. Appleby, *Env. This Mon.*, 1972, **1**, 29.
18 National Hydrogen Association. U.S. Department of Energy, *History of hydrogen*, 2010.
19 M. Carmo, D. L. Fritz, J. Mergel and D. Stolten, *Int. J. Hydrogen Energy*, 2013, **38**, 4901–4934.
20 H.-R. 'Molly' Jhong, S. Ma and P. J. Kenis, *Curr. Opin. Chem. Eng.*, 2013, **2**, 191–199.
21 D. T. Whipple and P. J. A. Kenis, *J. Phys. Chem. Lett.*, 2010, **1**, 3451–3458.
22 Fuel Cells and Hydrogen Joint Undertaking, *FCH JU Projects*, 2015.
23 T. Hua, R. Ahluwalia, L. Eudy, G. Singer, B. Jermer, N. Asselin-Miller, S. Wessel, T. Patterson and J. Marcinkoski, *J. Power Sources*, 2014, **269**, 975–993.
24 J. Alazemi and J. Andrews, *Renew. Sustain. Energy Rev.*, 2015, **48**, 483–499.
25 P. E. Dodds, I. Staffell, A. D. Hawkes, F. Li, P. Grünewald, W. McDowall and P. Ekins, *Int. J. Hydrogen Energy*, 2015, **40**, 2065–2083.
26 U.S. Department of Energy, *2014 Annual Progress Report*, 2015.
27 Mantra Energy, ERC Pilot Plant, http://mantraenergy.com/mantra-energy/technology/erc-pilot-plant/ , accessed 19/06/2015.
28 US Department of Energy, *An Integrated Strategic Plan for the Research, Development, and Demonstration of Hydrogen and Fuel Cell Technologies*, 2011.
29 Fuel Cells and Hydrogen Joint Undertaking, *Multi-Annual Work Plan 2014-2020*, 2014.
30 New Energy and Industrial Technology Development Organization (NEDO), *Development of fuel cells and hydrogen technologies*, 2009.
31 C. A. Rodriguez, M. A. Modestino, D. Psaltis and C. Moser, *Energy Environ. Sci.*, 2014, **7**, 3828–3835.
32 G. A. Olah, A. Goeppert and G. K. S. Prakash, *Beyond Oil and Gas: The Methanol Economy, Second updated and enlarged edition*, WILEY-VCH Verlag, Weinheim, 2nd edn., 2009.
33 K. Jüttner, in *Encyclopedia of Electrochemistry*, Wiley-VCH Verlag GmbH & Co. KGaA, 2007.
34 A. J. Bard and L. R. Faulkner, in *Electrochemical Methods: Fundamentals and Applications*, ed. 2nd, John Wiley & Sons, Inc., 2001, 44–86.
35 K. W. Harrison, R. Remick, G. D. Markin and A. Hoskin, in *18th World Hydrogen Energy Conference*, Essen, Germany, 2010.
36 H.-R. 'Molly' Jhong, F. R. Brushett and P. J. A. Kenis, *Adv. Energy Mater.*, 2013, **3**, 589–599.
37 E. Dufek, T. Lister and M. McIlwain, *J. Appl. Electrochem.*, 2011, **41**, 623–631.
38 T. Hatsukade, K. P. Kuhl, E. R. Cave, D. N. Abram and T. F. Jaramillo, *Phys. Chem. Chem. Phys.*, 2014, **16**, 13814–13819.
39 C. Delacourt, P. L. Ridgway, J. B. Kerr and J. Newman, *J. Electrochem. Soc.*, 2008, **155**, B42–B49.
40 S. Ma, R. Luo, S. Moniri, Y. Lan and P. J. A. Kenis, *J. Electrochem. Soc.*, 2014, **161**, F1124–F1131.
41 D. T. Whipple, E. C. Finke and P. J. A. Kenis, *Electrochem. Solid-State Lett.*, 2010, **13**, B109–B111.
42 H.-Y. Kim, I. Choi, S. H. Ahn, S. J. Hwang, S. J. Yoo, J. Han, J. Kim, H. Park, J. H. Jang and S.-K. Kim, *Int. J. Hydrogen Energy*, 2014, **39**, 16506–16512.
43 K. P. Kuhl, T. Hatsukade, E. R. Cave, D. N. Abram, J. Kibsgaard and T. F. Jaramillo, *J. Am. Chem. Soc.*, 2014, **136**, 14107–14113.
44 E. J. Dufek, T. E. Lister and M. E. McIlwain, *Electrochem. Solid-State Lett.* , 2012, **15** , B48–B50.
45 A. Awasthi, K. Scott and S. Basu, *Int. J. Hydrogen Energy*, 2011, **36**, 14779–14786.
46 F. Marangio, M. Santarelli and M. Cali, *Int. J. Hydrogen Energy*, 2009, **34**, 1143–1158.
47 Z. Liang, M. A. Ioannidis and I. Chatzis, *Chem. Eng. Sci.*, 2000, **55**, 5247–5262.
48 A. J. Bard and L. R. Faulkner, in *Electrochemical Methods: Fundamentals and Applications*, John Wiley and Sons, 2nd edn., 2001, 87–136.
49 E. A. Wargo, A. C. Hanna, A. Çeçen, S. R. Kalidindi and E. C. Kumbur, *J. Power Sources*, 2012, **197**, 168–179.
50 J. Xu, G. Liu, J. Li and X. Wang, *Electrochim. Acta*, 2012, **59**, 105–112.

51 J. Qiao, Y. Liu, F. Hong and J. Zhang, *Chem. Soc. Rev.*, 2014, **43**, 631–675.
52 C. Costentin, M. Robert and J.-M. Savéant, *Chem. Soc. Rev.*, 2013, **42**, 2423–2436.
53 J.-P. Jones, G. K. S. Prakash and G. A. Olah, *Isr. J. Chem.*, 2014, **54**, 1451–1466.
54 A. A. Peterson, F. Abild-pedersen, F. Studt, J. Rossmeisl and J. K. Nørskov, *Energy Environ. Sci.*, 2010, **3**, 1311–1315.
55 A. A. Peterson and J. K. Nørskov, *J. Phys. Chem. Lett.*, 2012, **3**, 251–258.
56 P. Hirunsit, *J. Phys. Chem. C*, 2013, **117**, 8262–8268.
57 E. Lamy, L. Nadjo and J. M. Saveant, *J. Electroanal. Chem. Interfacial Electrochem.*, 1977, **78**, 403–407.
58 Y. Chen, C. W. Li and M. W. Kanan, *J. Am. Chem. Soc.*, 2012, **134**, 19969–19972.
59 Z. M. Detweiler, J. L. White, S. L. Bernasek and A. B. Bocarsly, *Langmuir*, 2014, **30**, 7593–7600.
60 M. F. Baruch, J. E. Pander, J. L. White and A. B. Bocarsly, *ACS Catal.*, 2015, **5**, 3148–3156.
61 C. W. Li and M. W. Kanan, *J. Am. Chem. Soc.*, 2012, **134**, 7231–7234.
62 X. Feng, K. Jiang, S. Fan and M. W. Kanan, *J. Am. Chem. Soc.*, 2015, **137**, 4606–4609.
63 S. Rasul, D. H. Anjum, A. Jedidi, Y. Minenkov, L. Cavallo and K. Takanabe, *Angew. Chem. Int. Ed.*, 2015, **54**, 2146–50.
64 Y. Chen and M. W. Kanan, *J. Am. Chem. Soc.*, 2012, **134**, 1986–1989.
65 J. Medina-Ramos, R. C. Pupillo, T. P. Keane, J. L. DiMeglio and J. Rosenthal, *J. Am. Chem. Soc.*, 2015, **137**, 5021–5027.
66 B. A. Rosen, A. Salehi-Khojin, M. R. Thorson, W. Zhu, D. T. Whipple, P. J. A. Kenis and R. I. Masel, *Science.*, 2011, **334**, 643–644.
67 Y. Oh and X. Hu, *Chem. Soc. Rev.*, 2013, **42**, 2253–2261.
68 A. J. Morris, R. T. McGibbon and A. B. Bocarsly, *ChemSusChem*, 2011, **4**, 191–196.
69 E. Barton Cole, P. S. Lakkaraju, D. M. Rampulla, A. J. Morris, E. Abelev and A. B. Bocarsly, *J. Am. Chem. Soc.*, 2010, **132**, 11539–11551.
70 D. Gao, H. Zhou, J. Wang, S. Miao, F. Yang, G. Wang, J. Wang and X. Bao, *J. Am. Chem. Soc.*, 2015, **137**, 4288–4291.
71 A. Salehi-Khojin, H. R. M. Jhong, B. A. Rosen, W. Zhu, S. Ma, P. J. A. Kenis and R. I. Masel, *J. Phys. Chem. C*, 2013, **117**, 1627–1632.
72 R. Kas, R. Kortlever, H. Yılmaz, M. T. M. Koper and G. Mul, *ChemElectroChem*, 2015, **2**, 354–358.
73 R. Kortlever, I. Peters, S. Koper and M. T. M. Koper, *ACS Catal.*, 2015, **5**, 3916–3923.
74 H. Lim, H. Shin, W. A. Goddard, Y. J. Hwang, B. K. Min and H. Kim, *J. Am. Chem. Soc.*, 2014, **136**, 11355–11361.
75 J. Wu, F. G. Risalvato, P. P. Sharma, P. J. Pellechia, F.-S. Ke and X.-D. Zhou, *J. Electrochem. Soc.* , 2013, **160** , F953–F957.
76 A. Murata and Y. Hori, *Bull. Chem. Soc. Jpn.*, 1991, **64**, 123–127.
77 M. R. Thorson, K. I. Siil and P. J. A. Kenis, *J. Electrochem. Soc.*, 2013, **160**, F69–F74.
78 N. Gupta, M. Gattrell and B. MacDougall, *J. Appl. Electrochem.*, 2006, **36**, 161–172.
79 Y. Hori, A. Murata and R. Takahashi, *J. Chem. Soc. Faraday Trans. 1 Phys. Chem. Condens. Phases*, 1989, **85**, 2309–2326.
80 J. Wu, F. Risalvato and X.-D. Zhou, *ECS Trans.*, 2012, **41**, 49–60.
81 A. J. Bard and L. R. Faulkner, in *Electrochemical Methods: Fundamentals and Applications*, John Wiley and Sons, 2nd edn., 2001, 307–311.
82 ThyssenKroup Electrolysis GmbH, *Chlor-Alkali electrolysis plants. Superior membrane process*, 2013.
83 K. Hara, A. Kudo and T. Sakata, *J. Electroanal. Chem.*, 1995, **391**, 141–147.
84 M. Todoroki, K. Hara, A. Kudo and T. Sakata, *J. Electroanal. Chem.*, 1995, **394**, 199–203.
85 K. Hara, A. Tsuneto, A. Kudo and T. Sakata, *J. Electrochem. Soc.* , 1994, **141** , 2097–2103.
86 S. Ikeda, T. Takagi and K. Ito, *Bull. Chem. Soc. Jpn.*, 1987, **60**, 2517–2522.
87 K. Hirota, D. A. Tryk, T. Yamamoto, K. Hashimoto, M. Okawa and A. Fujishima, *J. Phys. Chem. B*, 1998, **102**, 9834–9843.
88 G. Zhao, T. Jiang, B. Han, Z. Li, J. Zhang, Z. Liu, J. He and W. Wu, *J. Supercrit. Fluids*, 2004, **32**, 287–291.
89 J. L. DiMeglio and J. Rosenthal, *J. Am. Chem. Soc.*, 2013, **135**, 8798–801.
90 E. Brunner, W. Hültenschmidt and G. Schlichthärle, *J. Chem. Thermodyn.*, 1987, **19**, 273–291.
91 T. Saeki, K. Hashimoto, A. Fujishima, N. Kimura and K. Omata, *J. Phys. Chem.*, 1995, **99**, 8440–8446.
92 T. Chang and R. W. Rousseau, *Fluid Phase Equilib.*, 1985, **23**, 243–258.
93 R. O'Hayre, D. M. Barnett and F. B. Prinz, *J. Electrochem. Soc.* , 2005, **152** , A439–A444.
94 U.S. Department of Energy, *Handbook of fuel cells*, U.S. Department of Energy, 7th edn., 2004.
95 A. Jayakumar, S. P. Sethu, M. Ramos, J. Robertson and A. Al-Jumaily, *Ionics*, 2015, **21**, 1–18.
96 S.-G. Kim and S.-J. Lee, *J. Power Sources*, 2013, **230**, 101–108.
97 E. J. Dufek, T. E. Lister, S. G. Stone and M. E. McIlwain, *J. Electrochem. Soc.*, 2012, **159**, F514–F517.
98 H. Wang and J. A. Turner, *J. Power Sources*, 2008, **183**, 576–580.
99 R. C. Weast, Ed., in *CRC Handbook of Chemistry, and Physics*, CRC Press, Boca Raton (Fla.), 70th edn., 1989, D–221.
100 D. Kopljar, A. Inan, P. Vindayer, N. Wagner and E. Klemm, *J. Appl. Electrochem.*, 2014, **44**, 1107–1116.
101 J. Gazzarri, M. Eikerling, Q. Wang and Z.-S. Liu, *Electrochem. Solid-State Lett.* , 2010, **13** , B58–B62.
102 J. W. Lim, Y.-H. Cho, M. Ahn, D. Y. Chung, Y.-H. Cho, N. Jung, Y. S. Kang, O.-H. Kim, M. J. Lee, M. Kim and Y.-E. Sung, *J. Electrochem. Soc.* , 2012, **159** , B378–B384.
103 M. S. Wilson and S. Gottesfeld, *J. Appl. Electrochem.*, 1992, **22**, 1–7.
104 X. Ren, M. S. Wilson and S. Gottesfeld, *J. Electrochem. Soc.* , 1996, **143** , L12–L15.
105 S. Zhang, X. Yuan, H. Wang, W. Merida, H. Zhu, J. Shen, S. Wu and J. Zhang, *Int. J. Hydrogen Energy*, 2009, **34**, 388–404.
106 J. Wu, X. Z. Yuan, J. J. Martin, H. Wang, J. Zhang, J. Shen, S. Wu and W. Merida, *J. Power Sources*, 2008, **184**, 104–119.
107 J. Chlistunoff, *Final report: Advanced Chlor-Alkali Technology. DOE Award 03EE-2F/ED190403*, 2005.
108 H.-Y. Jung and J. W. Kim, *Int. J. Hydrogen Energy*, 2012, **37**, 12580–12585.
109 O. Savadogo, *J. New Mater. Electrochem. Syst.*, 1998, **1**, 7–66.
110 P. Millet, *Int. J. Hydrogen Energy*, 1996, **21**, 87–93.
111 D. Wood, J. Davey, P. Atanassov and R. Borup, *ECS Trans.*, 2006, **3**, 753–763.
112 R. L. Borup, J. R. Davey, F. H. Garzon, D. L. Wood and M. A. Inbody, *J. Power Sources*, 2006, **163**, 76–81.
113 R. Borup, J. Davey, F. Garzon, D. Wood, P. Welch and K. More, *ECS Trans.*, 2006, **3**, 879–886.
114 J. Xie, D. L. Wood, K. L. More, P. Atanassov and R. L. Borup, *J. Electrochem. Soc.*, 2005, **152**, A1011–A1020.
115 S. Sharma and B. G. Pollet, *J. Power Sources*, 2012, **208**, 96–119.
116 L. M. Roen, C. H. Paik and T. D. Jarvi, *Electrochem. Solid-State Lett.* , 2004, **7** , A19–A22.
117 C. A. Reiser, L. Bregoli, T. W. Patterson, J. S. Yi, J. D. Yang, M. L. Perry and T. D. Jarvi, *Electrochem. Solid-State Lett.*, 2005, **8**, A273–A276.

118 F. Garzon, F. A. Uribe, T. Rockward, I. G. Urdampilleta and E. L. Brosha, *ECS Trans.*, 2006, **3**, 695–703.
119 Y. Hori, H. Konishi, T. Futamura, A. Murata, O. Koga, H. Sakurai and K. Oguma, *Electrochim. Acta*, 2005, **50**, 5354–5369.
120 N. Hoshi, T. Suzuki and Y. Hori, *J. Phys. Chem. B*, 1997, **101**, 8520–8524.
121 R. Kostecki and J. Augustynski, *Berichte der Bunsengesellschaft fur Phys. Chemie*, 1994, **98**, 1510–1515.
122 J. Lee and Y. Tak, *Electrochim. Acta*, 2001, **46**, 3015–3022.
123 G. V. Last and M. T. Schmick, *Identification and Selection of Major Carbon Dioxide Stream Compositions*, 2011.
124 V. Rosca, M. Duca, M. T. de Groot and M. T. M. Koper, *Chem. Rev.*, 2009, **109**, 2209–2244.
125 E. J. Dufek, T. E. Lister and M. E. McIlwain, *J. Electrochem. Soc.*, 2011, **158**, B1384–B1390.
126 K. Hara, A. Tsuneto, A. Kudo and T. Sakata, *J. Electroanal. Chem.*, 1997, **434**, 239–243.
127 US Department of Energy, *The Department of Energy Hydrogen and Fuel Cells Program Plan*, 2011.
128 D. W. DeWulf, *J. Electrochem. Soc.*, 1989, **136**, 1686–1691.
129 R. Shiratsuchi, Y. Aikoh and G. Nogami, *J. Electrochem. Soc.*, 1993, **140**, 3479–3482.
130 G. Nogami, H. Itagaki and R. Shiratsuchi, *J. Electrochem. Soc.*, 1994, **141**, 1138–1142.
131 A. M. Couper, D. Pletcher and F. C. Walsh, *Chem. Rev.*, 1990, **90**, 837–865.
132 Nancy L. Garland, T. G. Benjamin and John P. Kopasz, *Mater. matters*, 2008, **3**, 85–90.
133 M. Bodner, A. Hofer and V. Hacker, *Wiley Interdiscip. Rev. Energy Environ.*, 2014, **4**, 365–381.
134 K. Ayers, *PEM Electrolysis R&D Webinar*, DOE Fuel Cell Technologies Program Webinar2013.
135 D. Rakousky, C. Carmo, M. Stolten, in *227th ECS Meeting*, Chicago, Illinois USA, 2015.
136 A. Marshall, S. Sunde, M. Tsypkyn and R. Tunold, *Int. J. Hydrogen Energy*, 2007, **32**, 2320–2324.
137 K. Hara and T. Sakata, *Bull. Chem. Soc. Jpn.*, 1997, **70**, 571–576.
138 K. Manthiram, B. J. Beberwyck and A. P. Alivisatos, *J. Am. Chem. Soc.*, 2014, **136**, 13319–13325.
139 H. Yano, T. Tanaka, M. Nakayama and K. Ogura, *J. Electroanal. Chem.*, 2004, **565**, 287–293.
140 R. L. Cook, R. C. MacDuff and A. F. Sammells, *J. Electrochem. Soc.*, 1990, **137**, 607–608.
141 G. Arai, T. Harashina and I. Yasumori, *Chem. Lett.*, 1989, **18**, 1215–1218.
142 D. Ren, Y. Deng, A. D. Handoko, C. S. Chen, S. Malkhandi and B. S. Yeo, *ACS Catal.*, 2015, **5**, 2814–2821.
143 F. S. Roberts, K. P. Kuhl and A. Nilsson, *Angew. Chem. Int. Ed.*, 2015, **127**, 5268–5271.
144 Y. Momose, K. Sato and O. Ohno, *Surf. Interface Anal.*, 2002, **34**, 615–618.
145 E. Andrews, M. Ren, F. Wang, Z. Zhang, P. Sprunger, R. Kurtz and J. Flake, *J. Electrochem. Soc.*, 2013, **160**, H841–H846.
146 E. E. Barton, D. M. Rampulla and A. B. Bocarsly, *J. Am. Chem. Soc.*, 2008, **130**, 6342–6344.
147 G. Ghadimkhani, N. R. de Tacconi, W. Chanmanee, C. Janaky and K. Rajeshwar, *Chem. Commun.*, 2013, **49**, 1297–1299.
148 A. Bandi, *J. Electrochem. Soc.*, 1990, **137**, 2157–2160.
149 D. P. Summers, S. Leach and K. W. Frese, *J. Electroanal. Chem. Interfacial Electrochem.*, 1986, **205**, 219–232.
150 S. Litster and G. McLean, *J. Power Sources*, 2004, **130**, 61–76.
151 Y. Wang, K. S. Chen, J. Mishler, S. C. Cho and X. C. Adroher, *Appl. Energy*, 2011, **88**, 981–1007.
152 R. Zeis, *Beilstein J. Nanotechnol.*, 2015, **6**, 68–83.
153 L. Dubau, L. Castanheira, F. Maillard, M. Chatenet, O. Lottin, G. Maranzana, J. Dillet, A. Lamibrac, J.-C. Perrin, E. Moukheiber, A. ElKaddouri, G. De Moor, C. Bas, L. Flandin and N. Caqué, *Wiley Interdiscip. Rev. Energy Environ.*, 2014, **3**, 540–560.
154 A. A. Kulikovsky, *Electrochim. Acta*, 2010, **55**, 6391–6401.
155 M. Eikerling and A. A. Kornyshev, *J. Electroanal. Chem.*, 1998, **453**, 89–106.
156 T. Suzuki, H. Murate, T. Hatanaka and Y. Morimoto, *R&D Rev. Toyota CRDL*, 2004, **39**, 33–38.
157 H. Zhang, X. Wang, J. Zhang and J. Zhang, in *PEM Fuel Cell Electrocatalysts and Catalyst Layers*, ed. J. Zhang, Springer London, 2008, 889–916.
158 M. Lee, M. Uchida, H. Yano, D. A. Tryk, H. Uchida and M. Watanabe, *Electrochim. Acta*, 2010, **55**, 8504–8512.
159 E. Sadeghi, A. Putz and M. Eikerling, *J. Electrochem. Soc.* , 2013, **160** , F1159–F1169.
160 J. Marquis and M.-O. Coppens, *Chem. Eng. Sci.*, 2013, **102**, 151–162.
161 K. C. Neyerlin, W. Gu, J. Jorne, A. Clark and H. A. Gasteiger, *J. Electrochem. Soc.* , 2007, **154** , B279–B287.
162 S. H. Kim and H. Pitsch, *J. Electrochem. Soc.*, 2009, **156**, B673–B681.
163 E. Passalacqua, F. Lufrano, G. Squadrito, A. Patti and L. Giorgi, *Electrochim. Acta*, 2001, **46**, 799–805.
164 Q. Wang, H. Dong, H. Yu and H. Yu, *J. Power Sources*, 2015, **279**, 1–5.
165 A. Li, H. Wang, J. Han and L. Liu, *Front. Chem. Sci. Eng.*, 2012, **6**, 381–388.
166 J. Wu, P. P. Sharma, B. H. Harris and X. Zhou, *J. Power Sources*, 2014, **258**, 189–194.
167 L. You and H. Liu, *Int. J. Hydrogen Energy*, 2001, **26**, 991–999.
168 A. D. Le and B. Zhou, *Electrochim. Acta*, 2009, **54**, 2137–2154.
169 S. Mitchell, N.-L. Michels, K. Kunze and J. Pérez-Ramírez, *Nat. Chem.*, 2012, **4**, 825–831.
170 B. Bladergroen, H. Su, S. Pasupathi and V. Linkov, in *Electrolysis*, ed. J. Kepleris, InTech, 2012.
171 S. Ma, Y. Lan, G. M. J. Perez, S. Moniri and P. J. A. Kenis, *ChemSusChem*, 2014, **7**, 866–874.

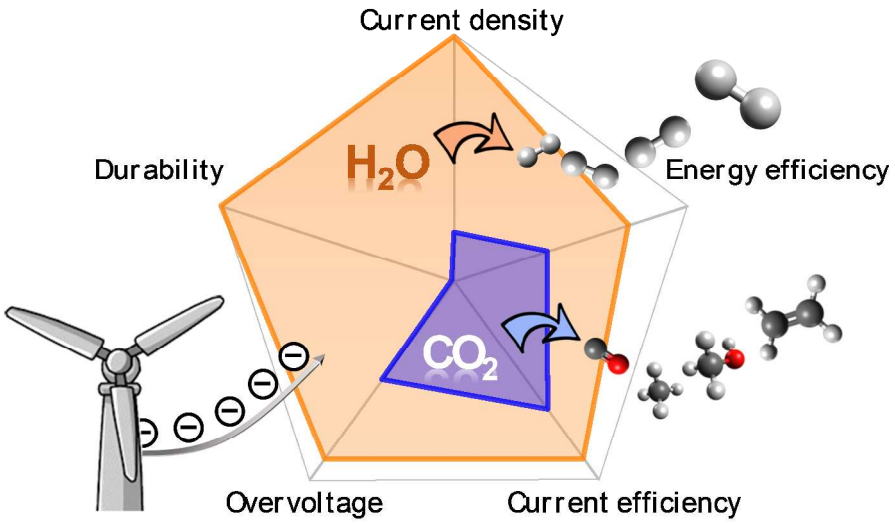

This Perspective discusses target parameters for the electroreduction of CO_2, based on its comparison with water splitting, to become a practical alternative for energy storage into fuels and chemicals.